Original Articles

Cancer-associated acinar-to-ductal metaplasia within the invasive front of pancreatic cancer contributes to local invasion

Shin Kibe[a], Kenoki Ohuchida[a,*], Yohei Ando[a], Shin Takesue[a], Hiromichi Nakayama[a], Toshiya Abe[a], Sho Endo[a], Kazuhiro Koikawa[a], Takashi Okumura[a], Chika Iwamoto[b], Koji Shindo[a], Taiki Moriyama[c], Kohei Nakata[a], Yoshihiro Miyasaka[a], Masaya Shimamoto[d], Takao Ohtsuka[a], Kazuhiro Mizumoto[d], Yoshinao Oda[e], Masafumi Nakamura[a,**]

[a] *Department of Surgery and Oncology, Graduate School of Medical Sciences, Kyushu University, Fukuoka, Japan*
[b] *Department of Advanced Medical Initiatives, Graduate School of Medical Sciences, Kyushu University, Fukuoka, Japan*
[c] *Department of Endoscopic Diagnostics and Therapeutics, Graduate School of Medical Sciences, Kyushu University, Fukuoka, Japan*
[d] *Kyushu University Hospital Cancer Center, Fukuoka, Japan*
[e] *Department of Anatomical Pathology, Graduate School of Medical Sciences, Kyushu University, Fukuoka, Japan*

ARTICLE INFO

ABSTRACT

The pancreas is an organ prone to inflammation, fibrosis, and atrophy because of an abundance of acinar cells that produce digestive enzymes. A characteristic of pancreatic cancer is the presence of desmoplasia, inflammatory cell infiltration, and cancer-associated acinar atrophy (CAA) within the invasive front. CAA is characterized by a high frequency of small ducts and resembles acinar-to-ductal metaplasia (ADM). However, the clinical significance of changes in acinar morphology, such as ADM with acinar atrophy, within the tumor microenvironment remains unclear. Here, we find that ADM within the invasive front of tumors is associated with cell invasion and desmoplasia in an orthotopic mouse model of pancreatic cancer. An analysis of resected human tumors revealed that regions of cancer-associated ADM were positive for TGFα, and that this TGFα expression was associated with primary tumor size and shorter survival times. Gene expression analysis identified distinct phenotypic profiles for cancer-associated ADM, sporadic ADM and chronic pancreatitis ADM. These findings suggest that the mechanisms driving ADM differ according to the specific tissue microenvironment and that cancer-associated ADM and acinar atrophy contribute to tumor cell invasion of the local pancreatic parenchyma.

1. Introduction

Pancreatic cancer remains one of the most lethal human cancers among all malignancies, with a 5-year survival rate of approximately 8% [1]. Pancreatic cancer is predicted to become the second leading cause of cancer mortality by the year 2030 [2]. Because the disease is commonly diagnosed at a late stage, less than 20% of patients present with localized, potentially curable tumors. Even after potentially curative resection, most patients will eventually have local recurrence. The biology of pancreatic cancer contributes to early recurrence and metastasis, and resistance to chemotherapy and radiotherapy [3]. Understanding the mechanisms underlying each phase of pancreatic cancer progression: initiation, invasion and metastasis, is therefore essential for the development of an effective diagnosis and treatments for this disease.

Pancreatic cancer is characterized by a dense stroma called desmoplasia, which plays a crucial role during tumor development [4,5]. The *LSL-Kras$^{G12D/+}$;LSL-Trp53$^{R172H/+}$;Pdx-1-Cre* (KPC) genetically engineered mouse model of pancreatic cancer faithfully recapitulating this histopathological feature of the human disease [6]. KPC mice therefore represent a potentially powerful tool to understand the pathophysiology of human pancreatic cancer [7]. However, in the primary tumors of KPC mice, unlike human pancreatic tumors, cancer cell invasion into the local pancreatic parenchyma is macroscopically and microscopically apparent before tumor cell dissemination or the formation of metastases. Such aggressive local invasion in the KPC mouse

model may result from the fact that these mice have been engineered to express oncogenic *Kras* in all types of pancreatic epithelia, including duct, acinar, and islet cells. In the KPC mouse model, a small number of dominant cancer cells invade a wide range of pancreatic parenchyma [8]. This suggests that, in contrast to the human pancreas, the pancreas of the KPC mouse, which is composed of acinar cells with *Kras* or *p53* mutation, provides a specific microenvironment conducive to the local invasion of pancreatic cancer cells within the pancreatic parenchyma.

Ductal lesions such as acinar-to-ductal metaplasia (ADM) are frequently observed in the pancreas of mice in which *PDX-1*-positive progenitor cells express oncogenic *Kras^{G12D}* [9–11]. In preliminary studies, we observed that ADM-like lesions frequently formed around the tumors of KPC mice. ADM induction is dependent upon the phenotypic plasticity of pancreatic acinar cells, and is accompanied by an altered gene expression, which includes a decrease in acinar markers, and the acquisition of ductal markers [12–14]. ADM is common in chronic pancreatitis where acinar atrophy and fibrosis are extensive [15,16]. ADM has been described in humans and mice, especially in the context of carcinogenesis [17,18]. Furthermore, in human pancreatic tissues, the surrounding acinar atrophy accompanying ADM is also associated with pancreatic intraepithelial neoplasia (PanIN), a precursor lesion of pancreatic cancer [19]. This suggests that acinar atrophy accompanying ADM is involved in pancreatic carcinogenesis associated with PanIN. We have previously observed acinar atrophy frequently associated with fibrosis remodeling in the invasive fronts of human and murine pancreatic tumors [20]. However, changes in acini morphology, such as acinar atrophy with ADM within the invasive front of a locally invasive tumor, have yet to be examined.

The aim of this study was to determine whether ADM exists within the invasive front of pancreatic cancer and whether the change in acinar morphology is associated with local tumor invasion. In human resected pancreatic cancer tissues, we observed ADM-like lesions in the invasive front of the tumor where acinar atrophy was apparent. We further demonstrate that cancer-associated ADM lesions induce desmoplasia and tumor cell invasion of the local parenchyma in a mouse model of pancreatic cancer. We demonstrate for the first time that ADM is a distinct characteristic of the invasive front in pancreatic cancer.

2. Materials and methods

Detailed information is provided in the Supplementary Materials and methods.

2.1. Human pancreatic tissues

Tissue samples were obtained from patients who underwent surgical resection for pancreatic cancer at Kyushu University Hospital. The study was approved by the Ethics Committee of Kyushu University and conducted according to the Ethical Guidelines for Human Genome/ Gene Research enacted by the Japanese Government and the Helsinki Declaration.

2.2. Immunohistochemistry

Human and mouse tissues were cut into 4-μm-thick sections and then subjected to hematoxylin and eosin (H&E) staining. In addition, immunohistochemistry was performed using rabbit anti-transforming growth factor alpha (TGFα; ab9585, Abcam, Cambridge, UK; 1:100 dilution), mouse anti-CK19 (sc-376126, Santa Cruz Biotechnology, Dallas TX, USA; 1:100 dilution), mouse anti-amylase (sc-46657, Santa Cruz Biotechnology; 1:100 dilution), or mouse anti-α-smooth muscle actin (αSMA) (#M0851, Dako, 1:100) primary antibody, followed by incubation with secondary antibody (En Vision System; K4002, Dako, Troy, MI, USA).

2.3. Cells and culture conditions

Human pancreatic stellate cell (PSC) lines were established from fresh surgical specimens of pancreatic cancer using the outgrowth method [21–23]. Pancreatic cancer cell (PCC) lines from the primary tumors of KPC mice were also established using an outgrowth method as described previously [24]. In addition, eleven other PCC lines were used in this study: SUIT-2, MIAPaCa-2 (Japanese Cancer Resource Bank, Osaka, Japan), Panc-1 (RIKEN BRC, Tsukuba, Japan), AsPC-1, SW1990, Capan-2, CFPAC-1, BxPC-3 (American Type Culture Collection, VA, USA), KP-3, H48N, and KP-2 (Dr. H. Iguchi, National Shikoku Cancer Center, Matsuyama, Japan). All PCC lines were obtained between 2011 and 2016, and propagated and frozen immediately after arrival. Cell lines were regularly authenticated by matched short tandem repeat DNA profiling. All cells were maintained as described previously [24].

2.4. Transgenic mouse models and in vivo experiments

The KPC and *LSL-Kras$^{G12D/+}$;Pdx-1-Cre* (KC) mouse models have been described previously [6,9]. Mice were genotyped by PCR using primers specific for transgenic alleles. KPC-derived PCCs (1×10^6) were orthotopically implanted into the tail of the pancreas of 7-week-old KC mice, which is before the formation of ADM in the host pancreatic parenchyma that results from the influence of *Kras^{G12D}* mutation. The mice were sacrificed on day 14 to exclude the possibility that acinar cells of the host pancreas change into cancerous lesions via multistep carcinogenesis. All orthotopic tumors, along with surrounding tissue, were excised and weighed. Tumor volume was calculated by the formula $\pi/6 \times (L \times W^2)$, where L is the largest tumor diameter and W is the smallest tumor diameter. All animal experiments were approved by the Ethics Committee of Kyushu University.

2.5. 3D culture of pancreatic acinar cells

For 3D explant cultures [25,26], cell culture plates were coated with collagen I in Waymouth's media. Isolated pancreatic acinar cells (PACs) were resuspended in a mixture of collagen I/Waymouth's media and added on the top of this layer. Waymouth's complete media was then added on top of the cell/gel mixture. The media was replaced the following day and then every other day during the course of explant culture. Ductal area was measured using ImageJ software at day four of explant culture.

2.6. Gene expression analysis

Gene expression was analyzed using the Mouse PanCancer Pathways Panel (XT−CSO−MPATH1-12) on the nCounter system (NanoString Technologies, Seattle, WA) [27] according to manufacturer's instructions. Raw data were normalized to the stable housekeeping gene, which was selected automatically by the system. The gene expression heatmap was generated in MultiExperiment Viewer version 4.9. Venn diagram analysis was performed using the VENNY tool (Bioinformatics for Genomics and Proteomics). Functional annotation clustering analysis was performed using the DAVID database (National Institute of Allergy and Infectious Diseases). Gene set enrichment analysis (GSEA) was performed for the three types of ADM by comparing expression data with that of normal acini. Comparisons were made by entering fold-change expression data from the nCounter analysis into the GSEA software (Broad Institute, UC San Diego) [28].

2.7. Statistical analysis

Data are represented as the mean ± standard deviation (SD). Comparisons between two groups were carried out using the Student's *t*-test, with a *P* value < 0.05 considered to be statistically significant.
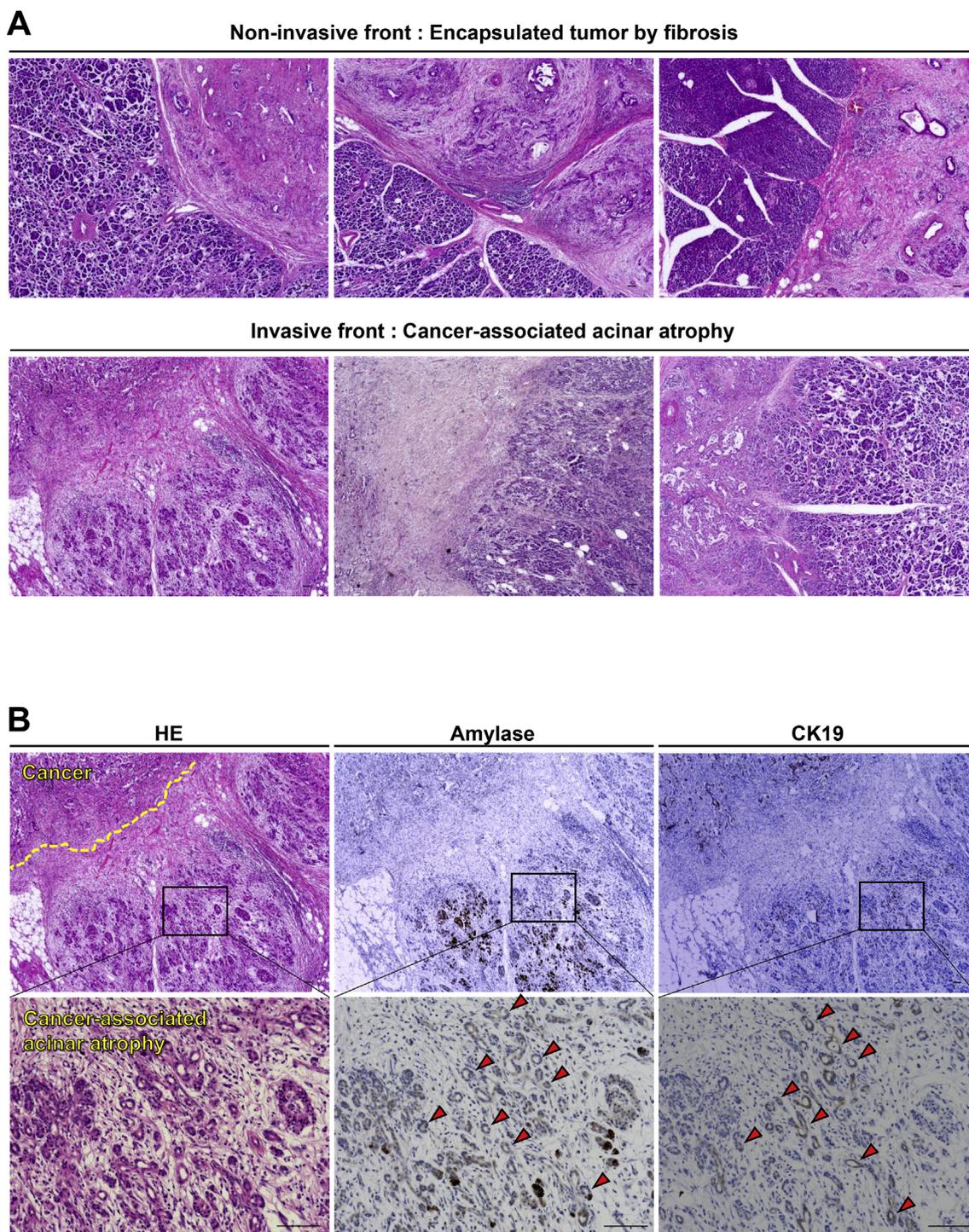
Fig. 1. ADM-like lesions are formed within the invasive front of pancreatic cancer. (A) Human pancreatic cancer samples stained with H&E. The border between the tumor and the acini can be divided into two histopathologically distinct regions, the invasive front and the non-invasive front. The invasive front is associated with CAA. In the non-invasive front, the tumor is encapsulated by fibrosis. (B) Immunohistochemical analysis of amylase and CK19 expression in serial sections of pancreatic cancer containing regions of CAA. Red arrowheads indicate the duct-like features of ADM stained with amylase and CK19. Scale bars, 100 μm.

The Kaplan–Meier method was used to analyze survival, with curves compared using the log-rank test. All statistical analyses were performed using JMP Pro 12 software (SAS Institute, Cary, NC, USA).

3. Results

3.1. ADM-like lesions are formed within the invasive front of pancreatic cancer

Histopathologically, the border between the tumor and the acini can be divided into two visibly distinct zones, the invasive front and the non-invasive front, as we have reported previously by collagen fiber analysis [20]. In the invasive front, cancer cells and/or cancer-
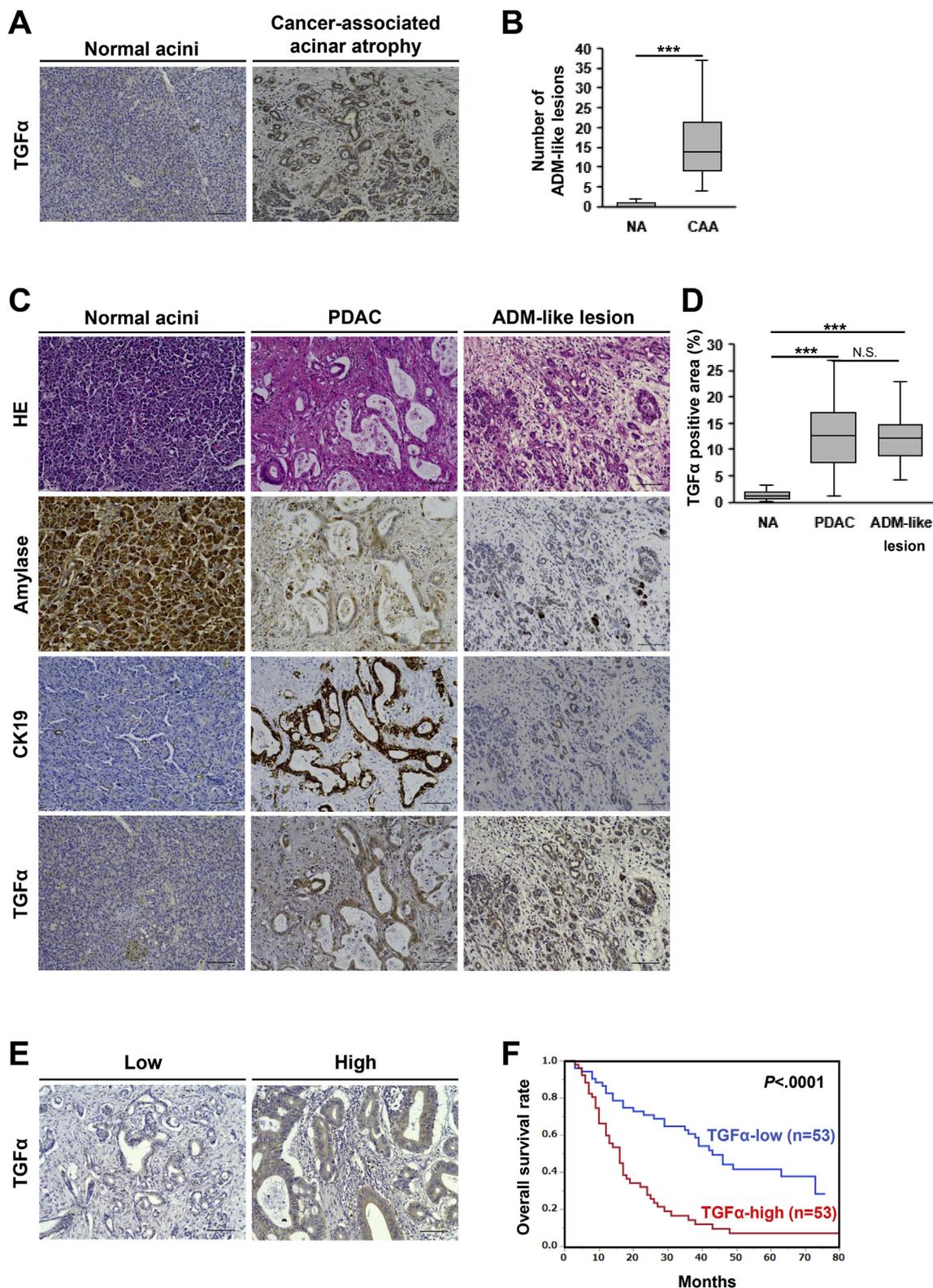
Fig. 2. TGFα is expressed in ADM-like lesions associated with CAA and is associated with poor prognosis. (A) Representative micrographs of TGFα staining in normal acini and regions of CAA. (B) ADM-like lesions positive for TGFα expression are found in regions of CAA ($n = 46$) but not in regions of normal acini ($n = 49$). (C) Representative micrographs of H&E, amylase, CK19 and TGFα staining in normal acini, pancreatic ductal adenocarcinoma (PDAC) and ADM-like lesion. (D) As with ADM-like lesions ($n = 46$), pancreatic cancer cells ($n = 106$) were positive for TGFα expression. (E) Representative immunohistochemistry images of pancreatic cancer tissue sections demonstrating low and high-intensity TGFα staining. (F) Kaplan–Meier analysis of overall survival according to TGFα expression in patients with pancreatic cancer ($n = 106$). TGFα expression was associated with shorter patient survival times. Data shown represent the mean ± SD. ***$P < 0.001$. Scale bars, 100 μm.

associated fibroblasts (CAFs) invade the pancreatic parenchyma. Acinar atrophy is frequently observed in this region while fibrotic encapsulation is uncommon. We define such acinar atrophy within the invasive front of pancreatic cancer as cancer-associated acinar atrophy (CAA). Within the non-invasive front, the tumor is encapsulated by fibrotic tissue and there are no cancer cells and CAFs invading the pancreatic parenchyma (Fig. 1A). Close examination of the CAA region within the invasive front revealed duct-like structures, which are similar to ADM (Fig. 1B). It is difficult to distinguish between small intra-acinar terminal ducts and ADM by morphology alone. Therefore, to confirm the origin of the duct-like structures within the invasive front, we performed immunohistochemistry for amylase and CK19 using serial sections of pancreatic tissues. The duct-like lesions stained positive for both amylase and CK19 (Fig. 1B), suggest that duct-like changes in acini such as ADM occur in the invasive front of pancreatic cancer. We define such duct-like changes in acini within the invasive front as cancer-associated ADM-like lesions. We next assessed the number of ADM-like lesions positive for TGFα expression (Fig. 2A). TGFα is a member of the epidermal growth factor (EGF) family of protein ligands, and transgenic mice overexpressing TGFα in the pancreas display multiple duct-like structures derived from differentiated acinar cells [29,30]. As expected, our analysis revealed that ADM-like lesions were positive for TGFα. Moreover, these lesions were frequently seen in regions of CAA, when compared with regions containing normal acini (Fig. 2B). Interestingly, as with the CAA region, the cancerous region was also positive for TGFα (Fig. 2C and D). We also evaluated TGFα expression in the cancer cells of 106 resected tumor samples. We divided pancreatic cancer patients into two groups according to the intensity of TGFα staining in cancer cells (Fig. 2E) and found that TGFα expression was associated with shorter postoperative survival times (Fig. 2F). Analysis of mRNA expression data from The Cancer Genome Atlas (TCGA) pancreatic cancer database also revealed that high *TGFA* gene expression was associated with shorter overall survival times (Fig. S1). TGFα expression was significantly associated with pathologic T category (Table 1), suggesting that TGFα is associated with the local progression of pancreatic cancer.

3.2. In KPC mice, tumor cell invasion into the local pancreatic parenchyma is extensive

To assess the mechanism driving cancer cell invasion into the local pancreatic parenchyma, we used KPC mice that recapitulate the clinical

Table 1
Relationship between TGFα expression and clinicopathologic factors.

Characteristics		TGFα low staining	TGFα high staining	P value
		n = 53 (50%)	n = 53 (50%)	
Age	< 65	24 (45.3)	18 (34.0)	.234
	≥65	29 (54.7)	35 (66.0)	
pT category	pT1/pT2	5 (9.4)	0 (0)	**.022**
	pT3/pT4	48 (90.6)	53 (100)	
pN category	pN0	12 (22.6)	10 (18.9)	.632
	pN1	41 (77.4)	43 (81.1)	
UICC stage	I/IIA	19 (35.8)	16 (30.2)	.536
	IIB/III/IV	34 (64.2)	37 (69.8)	
Histologic grade	G1/G2	44 (83.0)	43 (81.1)	.800
	G3	9 (17.0)	10 (18.9)	
pPL	No	50 (94.3)	49 (92.5)	.696
	Yes	3 (5.7)	4 (7.5)	
pPV	No	41 (77.4)	39 (73.6)	.652
	Yes	12 (22.6)	14 (26.4)	
pA	No	53 (100)	51 (96.2)	.153
	Yes	0 (0)	2 (3.8)	
Pathologic margin	Negative	40 (75.5)	35 (66.0)	.286
	Positive	13 (24.5)	18 (34.0)	

UICC, International Union Against Cancer.

and pathological features of human pancreatic cancer (Fig. 3C). In KPC mice, as with human pancreatic cancer, ADM-like ducts with acinar atrophy were seen in the invasive front of the tumor (Fig. 3B). Interestingly, the tumors of KPC mice demonstrated extensive local invasion, almost replacing the entirety of the pancreatic parenchyma, even before the formation of metastatic lesions (Fig. 3A). Indeed, there was no significant difference in primary tumor volume between KPC mice with or without metastasis and/or dissemination (Fig. 3D). There was also no significant difference in the overall survival rate between these two groups of mice (Fig. 3E).

3.3. Autocrine and paracrine effects of TGFα on pancreatic tumor, stellate and acinar cells

To investigate the autocrine and paracrine effects of TGFα in the tumor microenvironment, we examined the relative expression of this ligand and its cognate receptor, epidermal growth factor receptor (EGFR), in PCCs, PSCs and PACs, and we also determined the effects of TGFα treatment on the migratory and invasive behavior of these cells. TGFα and EGFR mRNA expression levels were measured in eleven PCC lines and three independent PSC primary cultures using qRT-PCR. All PCC lines exhibited higher levels of TGFα expression than the three PSC lines tested (Fig. 4A). Although relative TGFα expression was lower in PSCs, EGFR expression was detected in all cell lines tested (Fig. 4B). Both PCCs and PSCs exhibited a dose-dependent increase in migration and invasion in response to TGFα treatment (Fig. 4C and D).

Immunofluorescence analysis of primary mouse PACs revealed that these cells expressed amylase but not CK19 (Fig. 4E and F). To assess the effects of TGFα secreted by PCCs on the plasticity of PACs with or without *Kras^{G12D}* mutation, we performed an *in vitro* ADM assay. *Kras^{G12D}* PAC clusters exhibited greater changes in ductal morphological than *Kras^{WT}* clusters. Although changes in ductal morphology were observed in *Kras^{WT}* PAC clusters following treatment with TGFα, the effects of this ligand were more pronounced for the *Kras^{G12D}* clusters (Fig. 4G). Although, *Kras^{WT}* PAC clusters that were not treated with TGFα did not form a ductal structure, either TGFα treatment or *Kras^{G12D}* mutation resulted in the formation of large ductal structures that were similar to ADM (Fig. 4H).

3.4. ADM-dependent changes in acinar morphology contribute to pancreatic cancer cell invasion and desmoplasia

To investigate the effect of ADM on the local invasion of PCCs *in vivo*, we orthotopically transplanted KPC-derived PCCs into KC mice, a model in which ADM is commonly observed [9,10]. ADM-like ducts were frequently seen in the invasive front of tumors in *Kras^{G12D/+}* mice, as determined by histopathologic analysis. However, the histological appearance of the tumor core did not differ between *Kras^{WT}* and *Kras^{G12D/+}* mice (Fig. 5A, S2A). Immunohistochemical analysis revealed that ADM-like ducts in *Kras^{G12D/+}* mice exhibited acinar-to-ductal changes, with increased expression of CK19 and decreased expression of amylase (Fig. 5A). Tumor volume was significantly enhanced in the *Kras^{G12D/+}* mice (Fig. 5B and C), which commonly exhibited ADM within the invasive front. Liver metastasis and peritoneal dissemination were not detected in either *Kras^{WT}* or *Kras^{G12D/+}* mice (Table 2). We then examined the extent of desmoplasia in the invasive front of tumors. The desmoplastic area, identified by positive staining for αSMA, Sirius red and Masson trichrome, was significantly increased around the ADM-like ducts in *Kras^{G12D/+}* mice (Fig. 5D and E). Similar observations were made for the other KPC-derived PCCs (Figs. S2B, S2C, S2D). These findings suggest that the morphological changes in acini resulting from ADM-like lesions contribute to desmoplasia and the local invasion of pancreatic cancer *in vivo*.
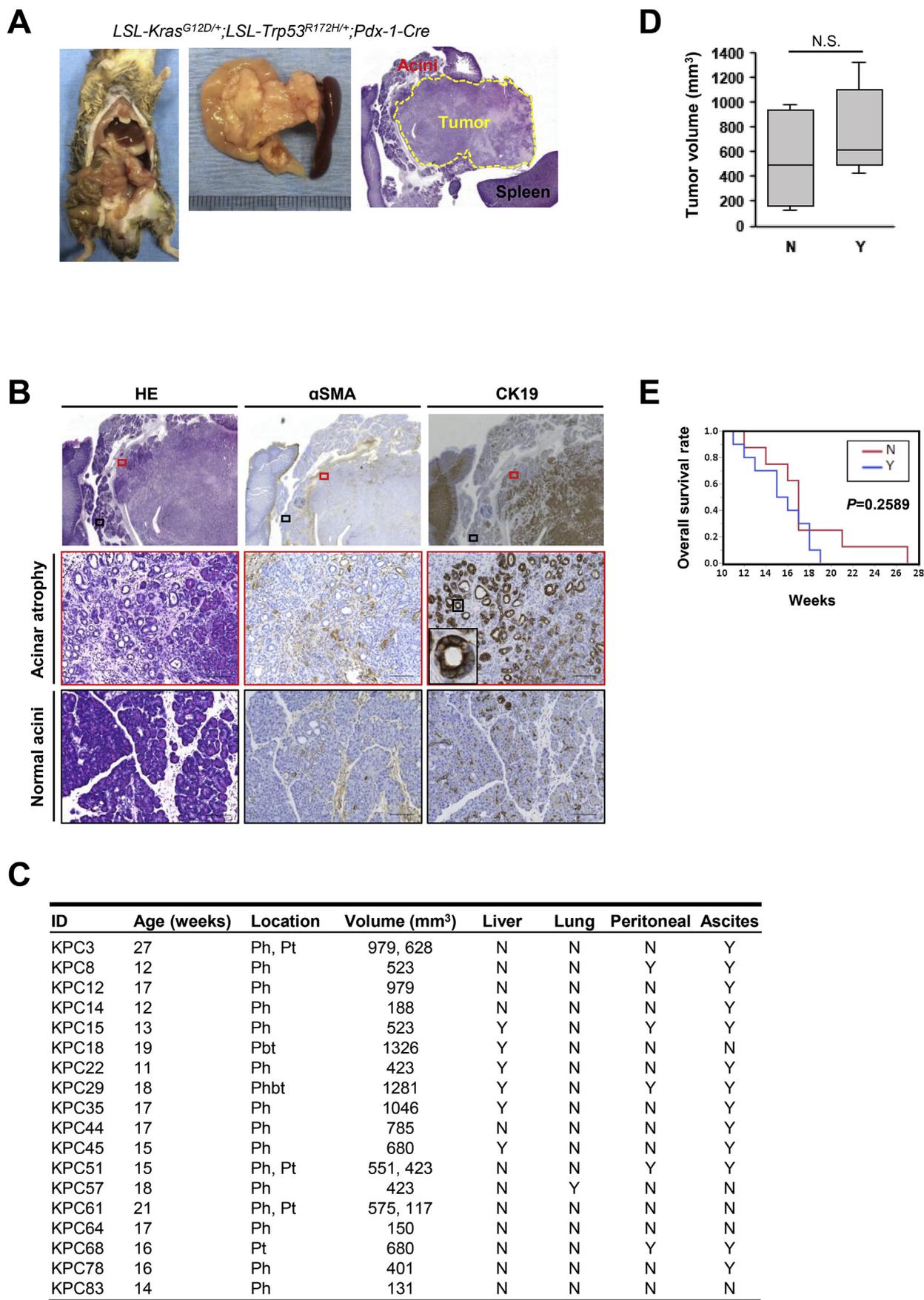
A *LSL-Kras^{G12D/+};LSL-Trp53^{R172H/+};Pdx-1-Cre*

D

B

E

C

ID	Age (weeks)	Location	Volume (mm³)	Liver	Lung	Peritoneal	Ascites
KPC3	27	Ph, Pt	979, 628	N	N	N	Y
KPC8	12	Ph	523	N	N	Y	Y
KPC12	17	Ph	979	N	N	N	Y
KPC14	12	Ph	188	N	N	N	Y
KPC15	13	Ph	523	Y	N	Y	Y
KPC18	19	Pbt	1326	Y	N	N	N
KPC22	11	Ph	423	Y	N	N	Y
KPC29	18	Phbt	1281	Y	N	Y	Y
KPC35	17	Ph	1046	Y	N	N	Y
KPC44	17	Ph	785	N	N	N	Y
KPC45	15	Ph	680	Y	N	N	Y
KPC51	15	Ph, Pt	551, 423	N	N	Y	Y
KPC57	18	Ph	423	N	Y	N	N
KPC61	21	Ph, Pt	575, 117	N	N	N	N
KPC64	17	Ph	150	N	N	N	N
KPC68	16	Pt	680	N	N	Y	Y
KPC78	16	Ph	401	N	N	N	Y
KPC83	14	Ph	131	N	N	N	N

Fig. 3. KPC mice demonstrate extensive cancer cell invasion into the local pancreatic parenchyma. (A) Representative photos and a photomicrograph of KPC mouse tumors. (B) Immunohistochemistry analysis of regions of cancer-associated acinar atrophy reveals CK19-positive duct-like structures with αSMA-positive desmoplasia. Scale bars, 100 μm. (C) Clinical findings for KPC mice summarizing the presence or absence of metastasis, peritoneal dissemination, and ascites. (D) Primary tumor volume was not associated with metastasis and/or dissemination. (E) Overall survival was not associated with metastasis and/or dissemination.
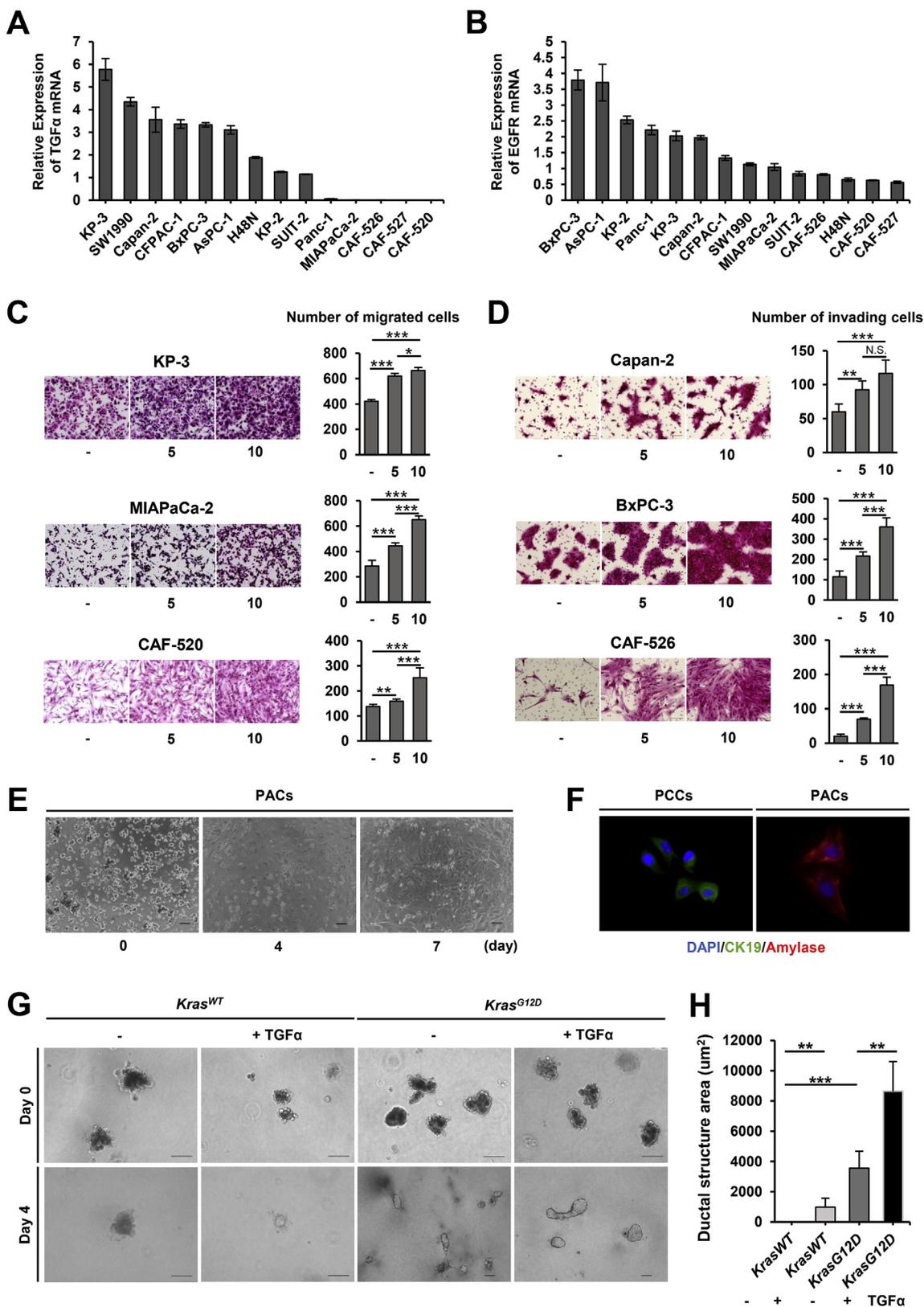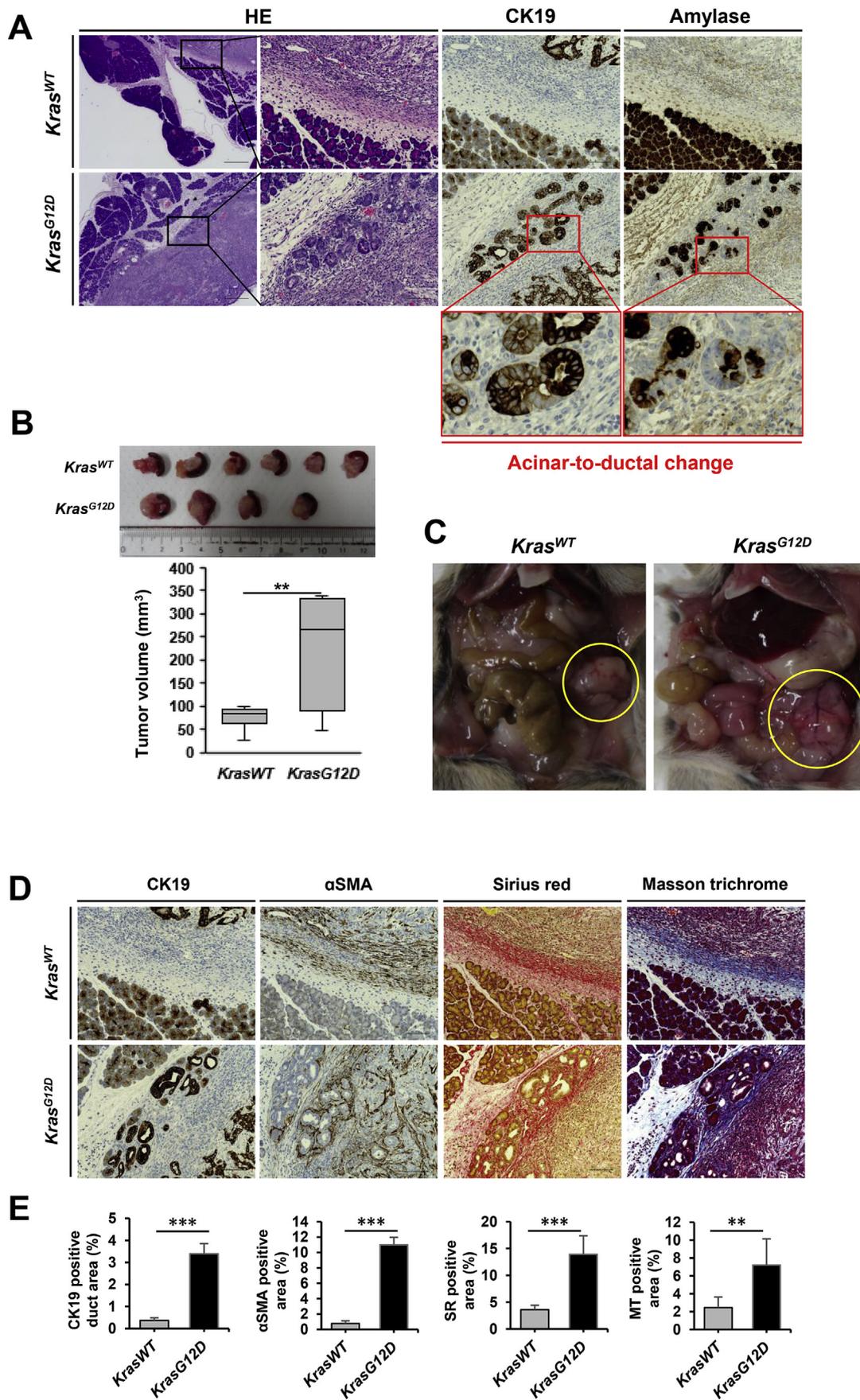
Fig. 4. Autocrine and paracrine effects of TGFα on the tumor microenvironment. (A) TGFα mRNA expression in PCCs and CAFs as determined by qRT-PCR. (B) EGFR mRNA expression in PCCs and CAFs as determined by qRT-PCR. (C) Representative microphotographs of H&E staining of migrating PCCs and CAFs treated with or without TGFα (5 or 10 ng/ml). (D) Representative microphotographs of H&E staining of invading PCCs and CAFs treated with or without TGFα (5 or 10 ng/ml). (E) Representative bright-field images of PACs cultured on type I collagen-coated dishes. Images were acquired after 0, 4, and 7 days in culture. (F) Immunofluorescence analysis confirmed that PACs expressed amylase but were negative for the PCC-marker CK19. (G) Primary acinar cells were isolated from *Kras*^{WT} or *Kras*^{G12D} mouse pancreas and cultured as 3D explants in collagen in the presence or absence of TGFα to determine the effects on duct formation. Acinar-to-ductal changes were associated with TGFα treatment and *Kras* mutation. (H) Quantification of ductal area. Data shown represent the mean ± SD. *$P < 0.05$, **$P < 0.01$, ***$P < 0.001$. Scale bars, 100 μm.

A
HE | CK19 | Amylase

Kras^WT

Kras^G12D

Acinar-to-ductal change

B

Kras^WT

Kras^G12D

Tumor volume (mm³)

**

KrasWT KrasG12D

C

Kras^WT | Kras^G12D

D
CK19 | αSMA | Sirius red | Masson trichrome

Kras^WT

Kras^G12D

E

CK19 positive duct area (%)

***

KrasWT KrasG12D

αSMA positive area (%)

***

KrasWT KrasG12D

SR positive area (%)

***

KrasWT KrasG12D

MT positive area (%)

**

KrasWT KrasG12D

(caption on next page)

Fig. 5. Pancreatic acinar conversion to ADM-like lesions within the invasive front induces the local invasion of pancreatic cancer cells and desmoplasia in murine orthotopic transplantation models. (A) Immunohistochemical analysis of ADM-like lesions within the invasive front of $Kras^{G12D}$ mice showing increased CK19 expression and decreased amylase expression associated with acinar-to-ductal change. Red-framed images highlight examples of ADM-like lesions. (B) Two weeks after orthotopic transplantation of KPC-derived PCCs, tumor volume in $Kras^{G12D}$ mice was significantly larger than that in $Kras^{WT}$ mice. (C) Representative photographs of the abdomen 2 weeks after implantation; yellow circles show pancreatic tumors. (D) Representative microphotographs of orthotopic tumor sections showing CK19, αSMA, Sirius red and Masson trichrome staining. (E) CK19-positive ADM-like lesions are surrounded by areas of desmoplasia, as determined by αSMA, Sirius red and Masson trichrome staining. Data shown represent the mean ± SD. **$P < 0.01$, ***$P < 0.001$. Scale bars for images in the left-hand column of A = 500 μm. All other scale bars = 100 μm. (For interpretation of the references to colour in this figure legend, the reader is referred to the Web version of this article.)

3.5. ADM is classified into three phenotypical subtypes that are determined by the tissue microenvironment

To further characterize the ADM phenotype associated with different pathological conditions, we performed gene expression analyses of tissues associated with three distinct forms of ADM by RNA sequencing (RNA-seq). Laser-capture microdissection (LCM) was used to capture tissues containing regions of cancer-associated ADM (CA-ADM) from the invasive front of pancreatic cancers, from pancreas with chronic pancreatitis-associated ADM (CP-ADM), and from pancreas with sporadic-ADM (SP-ADM) (Fig. 6A). Total RNA was isolated from the captured tissues, and the expression of 770 genes from 13 cancer-associated canonical pathways were subsequently analyzed using the NanoString nCounter gene expression system [27]. The heatmap analysis revealed that CA-ADM, CP-ADM, and SP-ADM exhibit distinct phenotypical gene expression profiles (Fig. 6B). Venn diagram analysis identified both differentially and co-expressed genes (Fig. 6C). In our analysis of the RNA-seq data, we found functional annotation clusters of genes uniquely up or down-regulated in each of the three types of ADM, when compared with normal acini (Fig. 6D). For each ADM subtype, representative genes with a fold change > 2 or < 0.5 were identified (Fig. S3B). In particular, growth factor, cytokine, and secretory factor-related genes were up-regulated in CA-ADM. Inflammatory response related genes were up-regulated in CP-ADM. Differentiation-related genes were up-regulated in all three subtypes of ADM. Apoptosis-related genes were up-regulated in both CA-ADM and CP-ADM. However, SP-ADM did not exhibit significant changes that were unique from the others forms of ADM (Fig. 6D). Additionally, GSEA analysis revealed that, when compared with normal acinar tissues, CA-ADM exhibited an up-regulation of pancreatic cancer-related genes, CP-ADM exhibited an up-regulation of inflammatory response genes, and SP-ADM revealed an up-regulation of genes associated with carcinogenesis (Fig. S3A). These results suggest the possibility that the mechanisms driving ADM differ according to the given tissue microenvironment.

4. Discussion

The pancreas is an organ in which inflammation, fibrosis and atrophy are easily induced because most of the pancreatic parenchyma is composed of acini that produce digestive enzymes [31]. However, the significance of the changes in acinar morphology within the surrounding microenvironment of the tumor during the development and progression of pancreatic cancer are unknown. In this study, we have found that the border between the tumor and the acini is largely divided into two histopathologically distinct regions, the invasive front and the non-invasive front. In the invasive front, cancer cells and/or CAFs demonstrate extensive invasion of the pancreatic parenchyma that is accompanied by desmoplastic changes and acinar atrophy. In the

non-invasive front, cancer cells and areas of desmoplasia are encapsulated by fibrosis. We also found extensive ADM-like lesions in areas of CAA observed within the invasive front of pancreatic tumors in both humans and KPC mice. In the orthotopic transplantation model, we also observed extensive ADM-like lesions and desmoplastic changes within the invasive front of tumors in the pancreas of mice. Furthermore, tumor volumes were also significantly larger, possibly because of the extensive ADM found in $Kras^{G12D/+}$ mice. These results suggest that ADM-like lesions within CAA regions of the invasive front enhance tumor invasion into the local pancreatic parenchyma.

Pancreatic acinar cells show plasticity termed ADM [12–14]. In previous reports, ADM has been described in humans and mice, especially regarding carcinogenesis [17,18], [32,33]. In our study, ADM-like lesions were observed in the invasive front, especially where acinar atrophy and invasion into the pancreatic parenchyma were extensive. In addition, a strong desmoplastic reaction was observed around these ADM-like lesions. When we induced temporary acute pancreatitis by administration of caerulein in KPC mice that had already formed palpable invasive cancer, tumor progression was accelerated (data not shown). This is possibly a consequence of the Kras mutation, which promotes ADM within the pancreas around the established tumor. Changes in the physical structural of the surrounding tumor microenvironment, including collagen matrix remodeling within regions of desmoplasia, are known to contribute to the process of cancer invasion [20,34]. These data suggest that ADM-like lesions with acinar atrophy and associated areas of desmoplasia within the invasive front of the tumor contribute to the formation of a microenvironment that favors local invasion in pancreatic cancer.
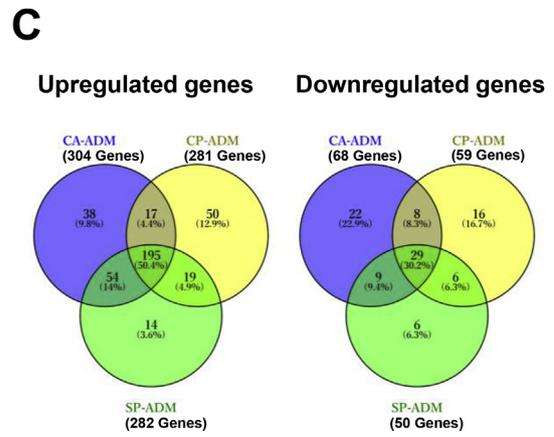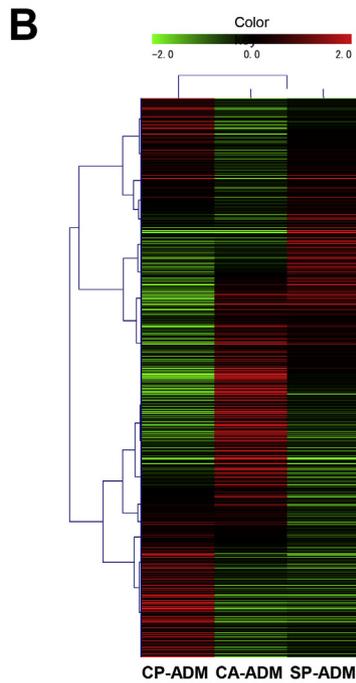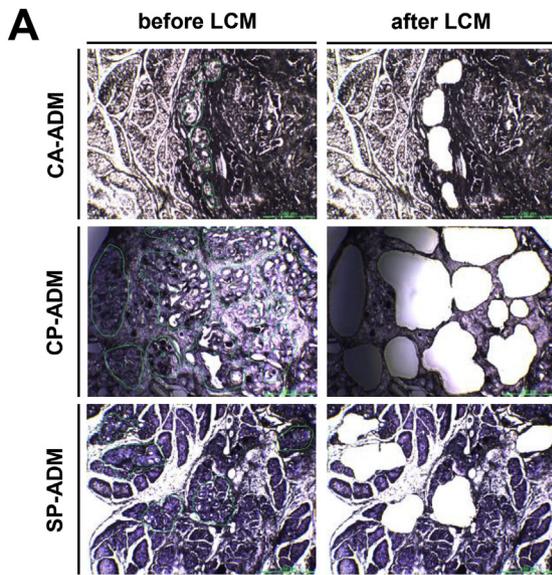
Several mechanisms linking ADM to carcinogenesis have been described [18,35], but the significance of ADM within the invasive front of the tumor has remained unclear. It has been reported that factors secreted by cancer cells, such as TGFα and TGFβ, are involved in ADM formation [17,36]. Our immunohistochemical analysis revealed that ADM lesions within the invasive front of the tumor were positive for TGFα expression. In addition, when PACs were stimulated with TGFα in an *in vitro* 3D explant culture model, they formed ADM-like structures. ADM can also be induced following pancreatic inflammation [37] and in response to macrophage-secreted cytokines [16]. Our present findings suggest that ADM can be classified according to three distinct phenotypical profiles that are dependent upon the properties of the local pancreatic microenvironment.

The *Klf4* gene, which is known to be essential for the induction of ADM [35,38], was up-regulated in all three subtypes of ADM. In CA-ADM, growth factor, cytokine, and secretory factor-related genes, such as *Bmp*, *Fgf*, *Il*, *Tnf* and *Mmp*, were up-regulated. Bone morphogenetic protein belongs to the TGFβ superfamily and has been implicated in the invasion and metastasis of cancer cells during epithelial–mesenchymal transition [39]. Fibroblast growth factor and Interleukin are

Table 2
Effects of *Kras* mutation on ADM-associated changes in acini in the orthotopic pancreatic cancer models employed in this study.

Group	Pancreatic tumor	Tumor volume (mm3)	Liver metastasis	Peritoneal dissemination	Body weight (g)
KrasWT (♂5, ♀7)	12/12	82.1 ± 40.6	0/12	0/12	27.88 ± 4.99
KrasG12D (♂5, ♀3)	8/8	258.2 ± 112.4	0/12	0/8	31.06 ± 7.4

A

	before LCM	after LCM
CA-ADM		
CP-ADM		
SP-ADM		

C

Upregulated genes

CA-ADM (304 Genes) CP-ADM (281 Genes)

38 (9.8%) 17 (4.4%) 50 (12.9%) 195 (50.4%) 54 (14%) 19 (4.9%) 14 (3.6%)

SP-ADM (282 Genes)

Downregulated genes

CA-ADM (68 Genes) CP-ADM (59 Genes)

22 (22.9%) 8 (8.3%) 16 (16.7%) 29 (30.2%) 9 (9.4%) 6 (6.3%) 6 (6.3%)

SP-ADM (50 Genes)

B

Color Key
−2.0 0.0 2.0

CP-ADM CA-ADM SP-ADM

D

Functional Annotation Chart of Upregulated Genes

CA-ADM	**P-Value**
Growth factor (Bmp8a, Fgf22, Fgf8, Gdf6, Inhbb, Il12a, Il2, Lefty2)	1.3E-9
Cytokine (Fasl, Bmp8a, Gdf6, Ifna1, Ifng, Il12a, Il2, Lefty2, Tnf)	3.1E-8
Secreted factor (Angpt2, Bmp8a, Efna1, Fgf22, Fgf8, Mmp7, Mmp9)	1.3E-6
Apoptosis (Bax, E2f1, Fasl, Gzmb, Gdf6, Stk4)	1.1E-3

CP-ADM	
Proto-oncogene (Abl1, Myb, Pdgfra, Pdgfd, Ret)	9.0E-8
Inflammatory response (Mecom, Il15, Irak2, Nfe2l2, Pparg)	1.3E-2
Apoptosis (Mecom, Abl1, Casp9, Chek2, Mapk3, Map2k6, Pak7)	8.9E-7

SP-ADM	
Disulfide bond	4.9E-3
Cleavage on pair of basic residues	8.6E-3
Calcium	1.1E-2

Common to three types of ADM	
Secreted	9.0E-29
Cytokine	2.1E-9
Differentiation	1.7E-9
Activator (Klf4, Gata3, Gli1, Gli3, Trp53)	1.0E-3

Functional Annotation Chart of Downregulated Genes

CA-ADM	**P-Value**
Developmental protein (Bmp4, Creb3l1, Dvl3, Foxo4, Spry2)	9.5E-3
Stress response (Idh2, Pik3r1)	6.4E-2

CP-ADM	
Cyclin (Ccne1, Ccne2, Ccno)	3.5E-4
Cell division (Cdc25c, Ccne1, Ccne2, Ccno)	1.7E-3
Cell cycle (Cdc25c, Ccne1, Ccne2, Ccno)	7.4E-3

SP-ADM	
Growth arrest (Ddit3, Gas1)	4.0E-3
Developmental protein (Lfng, Lefty1, Wnt10b)	1.7E-2
Wnt signaling pathway (Ddit3, Wnt10b)	3.8E-2

E

Cancer associated-ADM (CA-ADM)
↑ Growth factor
↑ Cytokine
↑ Secreted factor
↑ Apoptosis

Chronic pancreatitis–ADM (CP-ADM)
↑ Inflammatory response
↑ Apoptosis

Sporadic-ADM (SP-ADM)

Acini Cancer cell ADM Desmoplasia
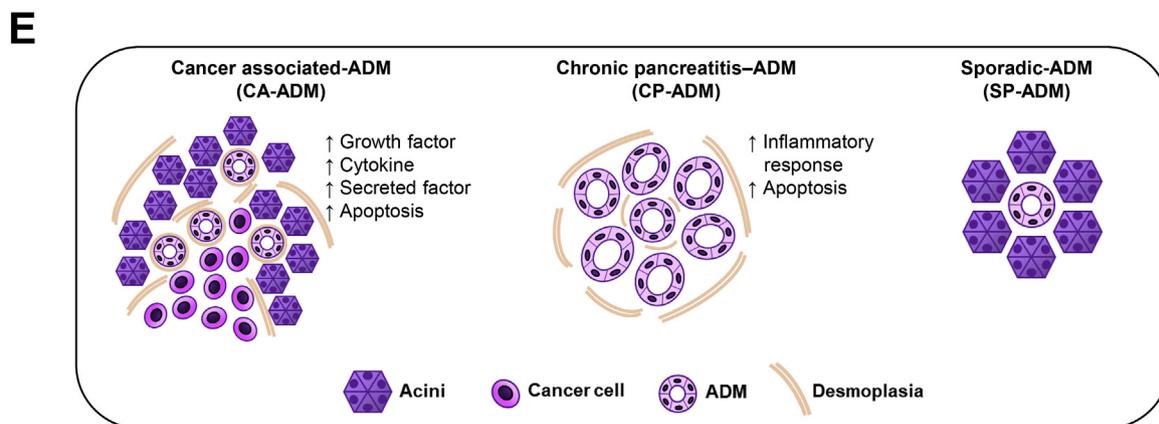
(caption on next page)

Fig. 6. ADM is associated with distinct phenotypical profiles that are determined by the specific tissue microenvironment. (A) Representative images of LCM. CA-ADM was derived from the invasive front of pancreatic cancer. CP-ADM was derived from chronic pancreatitis surrounded by inflammatory cells. SP-ADM was derived from regions of normal pancreas. Tissues from ADM lesions were captured from two cases of each ADM subtype. (B) Heatmap summarizing the results of the ADM gene expression analysis. Data represent log_2 fold changes in mean gene expression for each ADM subtype *vs.* normal acini. (C) Venn diagrams for differentially expressed genes (up or down-regulated) associated with each subtype of ADM. (D) Representative annotation chart of changes in gene expression (up or down-regulated) for the three subtypes of ADM. (E) Proposed model for ADM induction associated with different microenvironments.

extracellular signaling factors that regulate fibroblasts and inflammatory cells [40,41]. Tumor necrosis factor (TNF) activates NF-κB in acinar cells to induce the expression of numerous genes related to extracellular matrix degradation, ADM, and cancer cell invasion, such as matrix metalloproteinases (MMPs) [16, 34]. These data suggest that CA-ADM exerts effects on the surrounding microenvironment, impacting on various cell types including cancer cells, CAFs and inflammatory cells. In CP-ADM, inflammatory response-related genes, such as *Mecom*, *Il15* and *Nfe2l2*, were up-regulated, indicating that this subtype of ADM is induced by inflammation associated with pancreatitis. Interestingly, *Nfe2l2*, which is an anti-inflammatory gene that is associated with resentence responses to various forms of environmental stress [42,43], was up-regulated in addition to the inflammatory response genes. This suggests that CP-ADM is a defense mechanism induced to protect acinar cells from damage resulting from adverse conditions such as pancreatitis. However, CAF and inflammatory cell infiltration were not apparent features of SP-ADM, which is associated with a relatively normal microenvironment, suggesting that SP-ADM has less of an impact on the surrounding tissue. Further studies are now needed to understand the biological significance of, and molecular mechanisms associated with, the changes in gene expression observed for each specific subtype of ADM.

In conclusion, we have found that ADM lesions are associated with the invasive front of pancreatic cancer. The mechanism of ADM induction is dependent upon the characteristics of the local microenvironment. Such environmental factors can include interactions with cancer cells and infiltration by CAFs and/or inflammatory cells. CA-ADM, which exists within a tumor microenvironment, promotes desmoplastic changes and the invasion of cancer cells into the local pancreatic parenchyma. Our present data suggest that inhibition of ADM formation within the invasive front of the tumor may be a new therapeutic strategy to regulate the local invasion of pancreatic cancer.

Conflicts of interest

The authors declare no conflicts of interest.

Shin Kibe, Kenoki Ohuchida, Yohei Ando, Shin Takesue, Hiromichi Nakayama, Toshiya Abe, Sho Endo, Kazuhiro Koikawa, Takashi Okumura, Chika Iwamoto, Koji Shindo, Taiki Moriyama, Kohei Nakata, Yoshihiro Miyasaka, Masaya Shimamoto, Takao Ohtsuka, Kazuhiro Mizumoto, Yoshinao Oda, Masafumi Nakamura.

Appendix A. Supplementary data

Supplementary data to this article can be found online at https://doi.org/10.1016/j.canlet.2018.12.005.

References

[1] R.L. Siegel, K.D. Miller, A. Jemal, Cancer Statistics 66 (2016) 7–30, https://doi.org/10.3322/caac.21332 2016.

[2] L. Rahib, B.D. Smith, R. Aizenberg, A.B. Rosenzweig, J.M. Fleshman, L.M. Matrisian, Projecting cancer incidence and deaths to 2030: the unexpected burden of thyroid, liver, and pancreas cancers in the United States, Cancer Res. 74 (2014) 2913–2921, https://doi.org/10.1158/0008-5472.CAN-14-0155.

[3] D.P. Ryan, T.S. Hong, N. Bardeesy, Pancreatic adenocarcinoma, N. Engl. J. Med. 371 (2014) 1039–1049, https://doi.org/10.1056/NEJMra1404198.

[4] M.V. Apte, J.S. Wilson, A. Lugea, S.J. Pandol, A starring role for stellate cells in the pancreatic cancer microenvironment, Gastroenterology 144 (2013) 1210–1219, https://doi.org/10.1053/j.gastro.2012.11.037.

[5] M. Erkan, S. Hausmann, C.W. Michalski, A.A. Fingerle, M. Dobritz, J. Kleeff, H. Friess, The role of stroma in pancreatic cancer: diagnostic and therapeutic implications, Nat. Rev. Gastroenterol. Hepatol. 9 (2012) 454–467, https://doi.org/10.1038/nrgastro.2012.115.

[6] S.R. Hingorani, L. Wang, A.S. Multani, C. Combs, T.B. Deramaudt, R.H. Hruban, A.K. Rustgi, S. Chang, D.A. Tuveson, Trp53R172H and KrasG12D cooperate to promote chromosomal instability and widely metastatic pancreatic ductal adenocarcinoma in mice, Cancer Cell 7 (2005) 469–483, https://doi.org/10.1016/j.ccr.2005.04.023.

[7] P.K. Mazur, J.T. Siveke, Genetically engineered mouse models of pancreatic cancer: unravelling tumour biology and progressing translational oncology, Gut 61 (2012) 1488–1500, https://doi.org/10.1136/gutjnl-2011-300756.

[8] R. Maddipati, B.Z. Stanger, Pancreatic cancer metastases harbor evidence of polyclonality, Cancer Discov. 5 (2015) 1086–1097, https://doi.org/10.1158/2159-8290.CD-15-0120.

[9] S.R. Hingorani, E.F. Petricoin, A. Maitra, V. Rajapakse, C. King, M.A. Jacobetz, S. Ross, T.P. Conrads, T.D. Veenstra, B.A. Hitt, Y. Kawaguchi, D. Johann, L.A. Liotta, H.C. Crawford, M.E. Putt, T. Jacks, C.V.E. Wright, R.H. Hruban, A.M. Lowy, D.A. Tuveson, Preinvasive and invasive ductal pancreatic cancer and its early detection in the mouse, Cancer Cell 4 (2003) 437–450, https://doi.org/10.1016/S1535-6108(03)00309-X.

[10] J.P. Morris IV, D.A. Cano, S. Sekine, S.C. Wang, M. Hebrok, β-catenin blocks Kras-dependent reprogramming of acini into pancreatic cancer precursor lesions in mice, J. Clin. Invest. 120 (2010) 508–520, https://doi.org/10.1172/JCI40045.

[11] J.D. La O, L.L. Emerson, J.L. Goodman, S.C. Froebe, B.E. Illum, A.B. Curtis, L.C. Murtaugh, Notch and Kras Reprogram Pancreatic Acinar Cells to Ductal Intraepithelial Neoplasia vol. 105, (2008).

[12] A.V. Pinho, I. Rooman, M. Reichert, N. De Medts, L. Bouwens, A.K. Rustgi, F.X. Real, Adult pancreatic acinar cells dedifferentiate to an embryonic progenitor phenotype with concomitant activation of a senescence programme that is present in chronic pancreatitis, Gut 60 (2011) 958–966, https://doi.org/10.1136/gut.2010.225920.

[13] O. Basturk, S. Hong, L. Wood, N. Adsay, J. Albores-Saavedra, A. Biankin, L. Brosens, A revised classification system and recommendations from the baltimore consensus meeting for neoplastic precursor lesions in the pancreas, Am. J. Surg. Pathol. 39 (2016) 1730–1741, https://doi.org/10.1097/PAS.0000000000000533.A.

[14] P. Storz, Acinar cell plasticity and development of pancreatic ductal adenocarcinoma, Nat. Rev. Gastroenterol. Hepatol. 14 (2017) 296–304, https://doi.org/10.1038/nrgastro.2017.12.

[15] C. Guerra, A.J. Schuhmacher, M. Cañamero, P.J. Grippo, L. Verdaguer, L. Perez-Gallego, P. Dubus, E.P. Sandgren, M. Barbacid, Chronic pancreatitis is essential for induction of pancreatic ductal adenocarcinoma by K-ras oncogenes in adult mice, Cancer Cell 11 (2007) 291–302, https://doi.org/10.1016/j.ccr.2007.01.012.

[16] G.Y. Liou, H. Döppler, B. Necela, M. Krishna, H.C. Crawford, M. Raimondo, P. Storz, Macrophage-secreted cytokines drive pancreatic acinar-to-ductal metaplasia through NF-κB and MMPs, J. Cell Biol. 202 (2013) 563–577, https://doi.org/10.1083/jcb.201301001.

[17] G.Y. Liou, H. Döppler, K.E. DelGiorno, L. Zhang, M. Leitges, H.C. Crawford, M.P. Murphy, P. Storz, Mutant KRas-induced mitochondrial oxidative stress in acinar cells upregulates EGFR signaling to drive formation of pancreatic precancerous lesions, Cell Rep. 14 (2016) 2325–2336, https://doi.org/10.1016/j.celrep.2016.02.029.

[18] J.L. Kopp, G. von Figura, E. Mayes, F.F. Liu, C.L. Dubois, J.P. Morris, F.C. Pan, H. Akiyama, C.V.E. Wright, K. Jensen, M. Hebrok, M. Sander, Identification of sox9-dependent acinar-to-ductal reprogramming as the principal mechanism for initiation of pancreatic ductal adenocarcinoma, Cancer Cell 22 (2012) 737–750, https://doi.org/10.1016/j.ccr.2012.10.025.

[19] K. Brune, T. Abe, M. Canto, L. O'Malley, A.P. Klein, A. Maitra, N. Volkan Adsay, E.K. Fishman, J.L. Cameron, C.J. Yeo, S.E. Kern, M. Goggins, R.H. Hruban, Multifocal neoplastic precursor lesions associated with lobular atrophy of the pancreas in patients having a strong family history of pancreatic cancer, Am. J. Surg. Pathol. 30 (2006) 1067–1076 doi:pas.0000213265.84725.0b.

[20] K. Koikawa, K. Ohuchida, S. Takesue, Y. Ando, S. Kibe, H. Nakayama, S. Endo, T. Abe, T. Okumura, K. Horioka, M. Sada, C. Iwamoto, T. Moriyama, K. Nakata, Y. Miyasaka, R. Ohuchida, T. Manabe, T. Ohtsuka, E. Nagai, K. Mizumoto, M. Hashizume, M. Nakamura, Pancreatic stellate cells reorganize matrix components and lead pancreatic cancer invasion via the function of Endo180, Cancer Lett. 412 (2018) 143–154, https://doi.org/10.1016/j.canlet.2017.10.010.

[21] M.A.X.G. Bachem, E. Schneider, H. Groß, H. Weidenbach, R.M. Schmid, G. Adler, A. Menke, H. Siech, H. Beger, A. Gru, Identification, culture, and characterization of pancreatic stellate cells in rats and humans, Gastroenterology 115 (1998) 421–432.

[22] N. Ikenaga, K. Ohuchida, K. Mizumoto, L. Cui, T. Kayashima, K. Morimatsu, T. Moriyama, K. Nakata, H. Fujita, M. Tanaka, CD10+ pancreatic stellate cells enhance the progression of pancreatic cancer, Gastroenterology 139 (2010) 1041–1051, https://doi.org/10.1053/j.gastro.2010.05.084.

[23] S. Endo, K. Nakata, K. Ohuchida, S. Takesue, H. Nakayama, T. Abe, K. Koikawa, T. Okumura, M. Sada, K. Horioka, B. Zheng, Y. Mizuuchi, C. Iwamoto, M. Murata, T. Moriyama, Y. Miyasaka, T. Ohtsuka, K. Mizumoto, Y. Oda, M. Hashizume, M. Nakamura, Autophagy is required for activation of pancreatic stellate cells, associated with pancreatic cancer progression and promotes growth of pancreatic tumors in mice, Gastroenterology 152 (2017) 1492–1506, https://doi.org/10.1053/j.gastro.2017.01.010.

[24] K. Ohuchida, K. Mizumoto, M. Murakami, L. Qian, N. Sato, E. Nagai, K. Matsumoto, T. Nakamura, M. Tanaka, Radiation to stromal fibroblasts increases invasiveness of pancreatic cancer cells through tumor-stromal interactions, Gastroenterology 64 (2004) 3215–3222.

[25] C. Qu, S.F. Konieczny, Pancreatic acinar cell 3-dimensional culture, Bio Protoc 3 (2013).

[26] G.-Y. Liou, H. Döppler, U.B. Braun, R. Panayiotou, M.S. Buzhardt, D.C. Radisky, H.C. Crawford, A.P. Fields, N.R. Murray, Q.J. Wang, M. Leitges, P. Storz, Protein kinase D1 drives pancreatic acinar cell reprogramming and progression to intraepithelial neoplasia, Nat. Commun. 6 (2015), https://doi.org/10.1038/ncomms7200.

[27] G.K. Geiss, R.E. Bumgarner, B. Birditt, T. Dahl, N. Dowidar, D.L. Dunaway, H.P. Fell, S. Ferree, R.D. George, T. Grogan, J.J. James, M. Maysuria, J.D. Mitton, P. Oliveri, J.L. Osborn, T. Peng, A.L. Ratcliffe, P.J. Webster, E.H. Davidson, L. Hood, Direct multiplexed measurement of gene expression with color-coded probe pairs, Nat. Biotechnol. 26 (2008) 317–325, https://doi.org/10.1038/nbt1385.

[28] A. Subramanian, P. Tamayo, V.K. Mootha, S. Mukherjee, B.L. Ebert, M.A. Gillette, A. Paulovich, S.L. Pomeroy, T.R. Golub, E.S. Lander, J.P. Mesirov, Gene set enrichment analysis: a knowledge-based approach for interpreting genome-wide expression profiles, Proc. Natl. Acad. Sci. Unit. States Am. 102 (2005) 15545–15550, https://doi.org/10.1073/pnas.0506580102.

[29] M.B. Sporn, A.B. Roberts, Autocrine growth factors and cancer, Nature 313 (1985) 745–747, https://doi.org/10.1038/313745a0.

[30] E.P. Sandgren, N.C. Luetteke, R.D. Palmiter, R.L. Brinster, D.C. Leet, C. Hill, N. Carolina, Overexpression of TGFa in transgenic mice: induction of epithelial hyperplasia, pancreatic metaplasia, and carcinoma of the breast, Cell 61 (1990) 1121–1135.

[31] J. B, C.D. Logsdon, The role of protein synthesis and digestive enzymes in acinar cell injury, Nat. Rev. Gastroenterol. Hepatol. 10 (2013) 362–370, https://doi.org/10.1038/nrgastro.2013.36.The.

[32] C. Shi, S.-M. Hong, P. Lim, H. Kamiyama, M. Khan, R.A. Anders, M. Goggins, R.H. Hruban, J.R. Eshleman, KRAS2 mutations in human pancreatic acinar-ductal metaplastic lesions are limited to those with PanIN: implications for the human pancreatic cancer cell of origin, Mol. Canc. Res. 7 (2009) 230–236, https://doi.org/10.1158/1541-7786.MCR-08-0206.

[33] S. Hong, C.M. Heaphy, C. Shi, S. Eo, H. Cho, A.K. Meeker, J.R. Eshleman, R.H. Hruban, M. Goggins, Telomeres are shortened in acinar-to-ductal metaplasia lesions associated with pancreatic intraepithelial neoplasia but not in isolated acinar-to-ductal metaplasias, Mod. Pathol. 24 (2010) 256–266, https://doi.org/10.1038/modpathol.2010.181.

[34] P. Friedl, S. Alexander, Cancer invasion and the microenvironment: plasticity and reciprocity, Cell 147 (2011) 992–1009, https://doi.org/10.1016/j.cell.2011.11.016.

[35] D. Wei, L. Wang, Y. Yan, X. Kong, S. Huang, K. Xie, Z. Jia, M. Gagea, Z. Li, X. Zuo, KLF4 is essential for induction of cellular identity change and acinar-to-ductal reprogramming during early pancreatic carcinogenesis, Cancer Cell 29 (2016) 324–338, https://doi.org/10.1016/j.ccell.2016.02.005.

[36] J. Liu, N. Akanuma, C. Liu, A. Naji, G.A. Halff, W.K. Washburn, L. Sun, P. Wang, J.L. Kopp, M.A. Lipsett, M.L. Castellarin, L. Rosenberg, L. Zhu, G. Shi, C.M. Schmidt, R.H. Hruban, S.F. Konieczny, J.M. Bailey, K.E. DelGiorno, H.C. Crawford, G. Shi, J.P.D. La O, J.P. Morris, S.C. Wang, M. Hebrok, N. Habbe, N.M. Krah, S. Raimondi, A.B. Lowenfels, A.M. Morselli-Labate, P. Maisonneuve, R. Pezzilli, C. Guerra, C. Guerra, A.L. Means, G.-Y. Liou, J.T. Siveke, H.C. Crawford, G.-Y. Liou, N.-M. Chen, S.F. Boj, I. Houbracken, X. Xiao, J. Lee, C. Dorrell, W.A. Border, N.A. Noble, D. Pohlers, H.Y. Lan, Y. Fukumura, K. Suda, K. Mitani, M. Takase, T. Kumasaka, S.D. Slater, R.C. Williamson, C.S. Foster, J.L. Van Laethem, Y.E. Zhang, C.N. Street, T. Klein, M. Reichert, A.K. Rustgi, P.C. Konturek, T. Gress, K. Grabliauskaite, R.E. Wilentz, N. Bardeesy, K. Izeradjene, M.D. Molin, TGF-β1 promotes acinar to ductal metaplasia of human pancreatic acinar cells, Sci. Rep. 6 (2016) 30904, https://doi.org/10.1038/srep30904.

[37] O. Strobel, Y. Dor, J. Alsina, A. Stirman, G. Lauwers, A. Trainor, C.F. Del Castillo, A.L. Warshaw, S.P. Thayer, In vivo lineage tracing defines the role of acinar-to-ductal transdifferentiation in inflammatory ductal metaplasia, Gastroenterology 133 (2007) 1999–2009, https://doi.org/10.1053/j.gastro.2007.09.009.

[38] V.K. Xie, A. Maitra, Krüppel-like factor 4 promotes pancreatic acinar-to-ductal metaplasia and tumor initiation, Pancreas 46 (2017) 139–142, https://doi.org/10.1097/MPA.0000000000000773.

[39] D. Gonzalez, D. Medici, Signaling mechanisms of the epithelial-mesenchymal transition, Sci. Signal. 7 (2014) re8.

[40] M. Touat, E. Ileana, S. Postel-Vinay, F. André, J.C. Soria, Targeting FGFR signaling in cancer, Clin. Canc. Res. 21 (2015) 2684–2694, https://doi.org/10.1158/1078-0432.CCR-14-2329.

[41] D. Öhlund, A. Handly-Santana, G. Biffi, E. Elyada, A.S. Almeida, M. Ponz-Sarvise, V. Corbo, T.E. Oni, S.A. Hearn, E.J. Lee, I.I.C. Chio, C.-I. Hwang, H. Tiriac, L.A. Baker, D.D. Engle, C. Feig, A. Kultti, M. Egeblad, D.T. Fearon, J.M. Crawford, H. Clevers, Y. Park, D.A. Tuveson, Distinct populations of inflammatory fibroblasts and myofibroblasts in pancreatic cancer, J. Exp. Med. (2017), https://doi.org/10.1084/jem.20162024 jem.20162024.

[42] J.D. Hayes, A.T. Dinkova-Kostova, The Nrf2 regulatory network provides an interface between redox and intermediary metabolism, Trends Biochem. Sci. 39 (2014) 199–218, https://doi.org/10.1016/j.tibs.2014.02.002.

[43] E.L. Mills, D.G. Ryan, H.A. Prag, D. Dikovskaya, D. Menon, Z. Zaslona, M.P. Jedrychowski, A.S.H. Costa, M. Higgins, E. Hams, J. Szpyt, M.C. Runtsch, M.S. King, J.F. McGouran, R. Fischer, B.M. Kessler, A.F. McGettrick, M.M. Hughes, R.G. Carroll, L.M. Booty, E.V. Knatko, P.J. Meakin, M.L.J. Ashford, L.K. Modis, G. Brunori, D.C. Sévin, P.G. Fallon, S.T. Caldwell, E.R.S. Kunji, E.T. Chouchani, C. Frezza, A.T. Dinkova-Kostova, R.C. Hartley, M.P. Murphy, L.A. O'Neill, Itaconate is an anti-inflammatory metabolite that activates Nrf2 via alkylation of KEAP1, Nature 556 (2018) 113–117, https://doi.org/10.1038/nature25986.